Mon. Not. R. Astron. Soc. **374,** 1457–1472 (2007) doi:10.1111/j.1365-2966.2006.11290.x

Semi-empirical analysis of Sloan Digital Sky Survey galaxies – IV. A nature via nurture scenario for galaxy evolution

Abílio Mateus,[1⋆] Laerte Sodré, Jr,[1] Roberto Cid Fernandes[2] and Grażyna Stasińska[3]

[1]*Departamento de Astronomia, IAG-USP, Rua do Matão 1226, 05508-090 São Paulo, Brazil*
[2]*Departamento de Física - CFM - Universidade Federal de Santa Catarina, Florianópolis, SC, Brazil*
[3]*LUTH, Observatoire de Meudon, 92195 Meudon Cedex, France*

Accepted 2006 November 2. Received 2006 August 28; in original form 2006 March 28

ABSTRACT

We investigate the environmental dependence of stellar population properties of galaxies in the local Universe. Physical quantities related to the stellar content of galaxies are derived from a spectral synthesis method applied to a volume-limited sample containing more than 60 000 galaxies ($0.04 < z < 0.075$; $M_r \leqslant -19.9$), extracted from the Data Release 4 of the Sloan Digital Sky Survey. Mean stellar ages, mean stellar metallicities and stellar masses are obtained from this method and used to characterize the stellar populations of galaxies. The environment is defined by the projected local galaxy density estimated from a nearest neighbour approach. We recover the star formation–density relation in terms of the mean light-weighted stellar age, which is strongly correlated with star formation parameters derived from Hα. We find that the age–density relation is distinct when we divide galaxies according to luminosity or stellar mass. The relation is remarkable for galaxies in all bins of luminosity. On the other hand, only for an intermediate stellar mass interval (associated to a transition in galaxy properties) the relation shows a change in galaxy properties with environment. Such distinct behaviours are associated to the large stellar masses of galaxies with the same luminosity in high-density environments. In addition, the well-known star formation–density relation results from the prevalence of massive systems in high-density environments, independently of galaxy luminosity, with the additional observed downsizing in galaxy formation, in which the star formation is shifted from massive galaxies at early times to low-mass galaxies as the Universe evolves. Finally, our results support that a natural path for galaxy evolution proceeds *via* a nurture way, in the sense that galaxy evolution is accelerated in denser environments, that took place mainly at high redshifts.

Key words: stars: formation – galaxies: evolution – galaxies: formation – galaxies: fundamental parameters – galaxies: stellar content.

1 INTRODUCTION

Galaxy environment has a fundamental role in the evolutionary paths followed by galaxies. It is well known that galaxy populations change according to the environment in which they are found. The most classical evidence of such environmental dependence is the morphology–density relation (e.g. Dressler 1980; Whitmore, Gilmore & Jones 1993). The fraction of galaxies with distinct morphological types (essentially spirals, lenticulars and ellipticals) correlates strongly with the local galaxy density, with high-density environments being populated preponderantly by early-type galaxies. This is related to the dependence of the fraction of star-forming galaxies on the environment, based on the presence or absence of emission lines, such as Hα and [O II], in galaxy spectra (e.g. Hashimoto et al. 1998; Carter et al. 2001; Mateus & Sodré 2004). Such dependence is also intrinsically related to the reduced gaseous content of galaxies in denser regions (Solanes, Giovanelli & Haynes 1996; Bravo-Alfaro et al. 2000; Goto et al. 2003).

Recent studies have found that the star formation rate (SFR) of galaxies is the most-sensitive parameter to galaxy environment, declining strongly in high-density regions of galaxy clusters (e.g. Lewis et al. 2002; Gómez et al. 2003; Rines et al. 2005), whereas structural parameters are less affected by environment (Kauffmann et al. 2004). The environment–SFR relation has also an additional dependence on galaxy luminosity, being steeper for fainter galaxies (Tanaka et al. 2004). However, when one restricts the analysis to star-forming galaxies, the median SFR of this class of objects

⋆E-mail: abilio@astro.iag.usp.br

seems to be unaffected by environment, although the fraction of such galaxies decreases with increasing local density (Balogh et al. 2004).

The most plausible way to account for these trends is to assume that galaxy properties (mainly those related to star formation and gas properties) are affected by environment through well-known physical mechanisms acting on galaxies. This path, linked directly to the environment, gives origin to a *nurture* perspective for galaxy evolution. In fact, several physical mechanisms were already proposed and studied to account for the evolutionary trends discussed above. Interactions between the intragalactic and intergalactic medium, including gas removal and evaporation (*ram pressure stripping*; Gunn & Gott 1972; Fujita & Nagashima 1999; Vollmer et al. 2001), and the suppression of the accretion of gas-rich materials in the neighbourhood of the galaxy (*starvation*; Larson, Tinsley & Caldwell 1980; Bekki, Couch & Shioya 2001), are typical mechanisms claimed to affect star formation properties of galaxies infalling on to denser regions.

Another path by which galaxy evolution proceeds is related to the initial conditions established during the formation epoch of galaxies, which could, in principle, account for the relations between galaxy properties and environment. This path gives origin to a *nature* perspective driving galaxy evolution. As expected from a biased galaxy formation scenario (e.g. Cen & Ostriker 1993), massive galaxies are formed earlier preferentially in high-density regions; in opposition, low-mass galaxies would be formed later with a smooth distribution in the density field. Thus, in this scenario there is, naturally, an expected relation between age of formation (or mass) and environmental density. In fact, hierarchical galaxy formation models successfully reproduce the morphology–density relation (e.g. Benson et al. 2001), demonstrating that it is present even if the physical mechanisms mentioned above are not considered.

Additionally, studies based on high-redshift galaxies (e.g. Cowie et al. 1996; Kodama et al. 2004; Juneau et al. 2005, and others) and also on local galaxies (Kauffmann et al. 2003; Heavens et al. 2004; Mateus et al. 2006, hereafter SEAGal II) have revealed that the existence of a 'downsizing' in galaxy formation is extremely important in analysis involving the star formation properties of galaxies. These results suggest that massive galaxies have stopped to form stars at earlier times, with low-mass systems comprising a large fraction among galaxies with ongoing star formation. These trends are also recovered by recent high-resolution simulations (e.g. Weinberg et al. 2004) and semi-analytic models for galaxy formation (e.g. Menci et al. 2005; de Lucia et al. 2006). However, the physical origin of the downsizing is still a subject of debate (e.g. Scannapieco, Silk & Bouwens 2005; Bundy et al. 2006; de Lucia et al. 2006).

Here, we will shed some light into the discussion concerning galaxy formation and evolution by investigating the role of environment on the stellar population properties of galaxies in the nearby Universe. Other works have increased our understanding on this issue through distinct approaches (e.g. Kauffmann et al. 2004; Clemens et al. 2006; Poggianti et al. 2006; Thomas et al. 2005). In this paper, we will use the results of the application of a spectral synthesis method to a volume-limited sample of Sloan Digital Sky Survey (SDSS) galaxies. This method is able to recover important physical properties of galaxies from their spectra, including mean stellar ages, mean stellar metallicities and stellar masses, among others. The details of such approach were discussed by Cid Fernandes et al. (2005) (hereafter SEAGal I) and its results have been recently used in SEAGal II, where we have studied the bimodality of the galaxy population.

In this work, we show that the relations between galaxy properties and environment, well characterized by the age–density relation, are distinct when we divide galaxies according to luminosity or stellar mass. This is a result of the different mass-to-light ratios ($M_\star/L$s) of galaxies in distinct environments. In dense regions, galaxies of same luminosity tend to have higher $M_\star/L$. We argue that a natural path emerges from these results but via a nurture way in the sense that massive galaxies are formed preferentially in high-density regions (where the evolution was accelerated) in the high-z Universe (when the SFR was high), since their stellar populations also tend to be the oldest ones and they inhabit the densest regions we observe in the local Universe.

This paper is organized as follows. Section 2 describes the data used in this work, the galaxy sample definition and a brief overview of the spectral synthesis method used in our analysis. Section 3 describes some parameters related to star formation activity in galaxies that will be discussed in this work, and Section 4 defines the environmental parameter, namely the projected local galaxy density. In Section 5, we investigate the environmental dependence of the stellar population properties of galaxies. Finally, in Section 6, we discuss the implications of our findings in the context of galaxy evolution, and in Section 7 we summarize the main results of this work.

2 THE DATA

The data used in this work were extracted from the SDSS available publicly in its Data Release 4 (DR4; Adelman-McCarthy et al. 2006). The SDSS is an ambitious project planned to study the large-scale structure of the Universe as well as other relevant subjects of extragalactic astronomy. The survey aims to cover one-quarter of the entire sky (mainly in the Northern hemisphere) obtaining photometric information in five optical bands (u, g, r, i and z) for millions of objects and spectroscopic data for about 10^6 galaxies brighter than $r = 17.77$.

In this section, we describe the volume-limited sample of SDSS galaxies used in our analysis and the application of a spectral synthesis method to the spectroscopic data aiming to obtain some fundamental physical properties of galaxies in the local Universe. In this work, we use the following values of the cosmological parameters: $H_0 = 70$ km s^{-1} Mpc^{-1}, $\Omega_{\rm M} = 0.3$ and $\Omega_\Lambda = 0.7$.

2.1 Galaxy sample

We built a volume-limited sample of galaxies from the SDSS DR4. This sample follows the same criteria used by Strauss et al. (2002) to define the Main Galaxy Sample, consisting of galaxies with r-band Petrosian magnitudes $r \leqslant 17.77$ and r-band Petrosian half-light surface brightnesses $\mu_{50} \leqslant 24.5$ mag arcsec^2. We have selected galaxies with redshifts in the range $0.04 < z < 0.075$ with r-band extinction-corrected absolute magnitudes $M_r \leqslant -19.9$, corresponding roughly to $M_r^* + 1.5$. The absolute magnitudes adopted here are k-corrected by using the KCORRECT v3_2 code provided by Blanton et al. (2003c). The lower redshift limit was chosen here to avoid the undesirable presence of aperture effects in our analysis which are related to the use of small 3-arcsec fibres in the SDSS to obtain the spectroscopic data (Kewley, Jansen & Geller 2005). We have detected a minor fraction of galaxies with multiple spectral data, from which we have considered only those with best signal-to-noise ratio (S/N) in the g band. These selection criteria result in a volume-limited sample containing 63 659 galaxies.

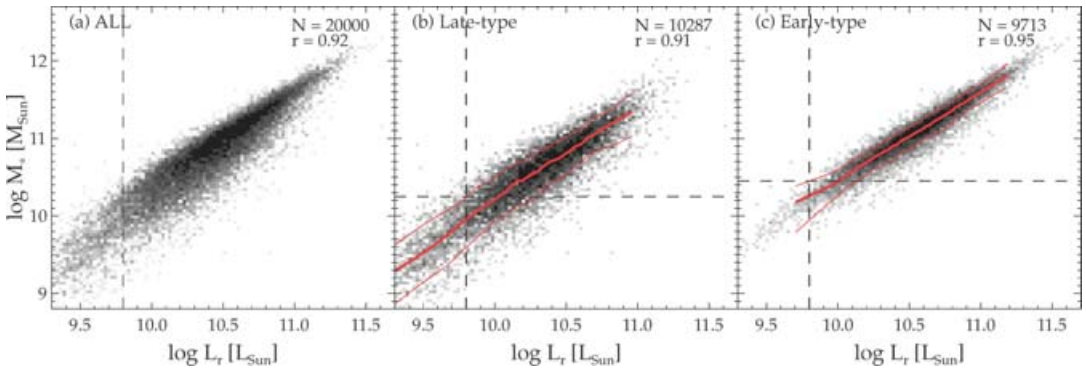

Figure 1. Mass–luminosity relation for (a) all galaxies in the 20 k sample, (b) late-type galaxies with $D_n(4000) < 1.67$ and (c) early-type galaxies with $D_n(4000) > 1.67$. The solid lines are the median values (thick lines) and 10–90 percentiles (thin lines) for the relations. The luminosity limit for our sample ($\log L_r/\mathrm{L}_\odot = 9.80$) is shown as the vertical dashed lines, while the mass values above which our sample will be considered complete are shown as the horizontal dashed lines. The numbers at the top right-hand panel are the count of galaxies in each panel and the Spearman correlation coefficient.

2.2 Overview of the spectral synthesis method

We used the STARLIGHT code (described in detail in SEAGal I and updated in SEAGal II) to obtain physical parameters of galaxies directly from their spectra (essentially from continuum and absorption lines). STARLIGHT fits an observed spectrum with a combination of $N_\star$ simple stellar populations (SSPs) from the evolutionary synthesis models of Bruzual & Charlot (2003). Here, we used a base containing $N_\star = 150$ elements, spanning six metallicities – $Z = 0.005$, 0.02, 0.2, 0.4, 1 and 2.5 $\mathrm{Z}_\odot$ – and 25 ages, between 1 Myr and 18 Gyr. Stellar extinction is modelled as due to foreground dust, with the extinction law of Cardelli, Clayton & Mathis (1989) with $R_V = 3.1$, and parametrized by the V-band extinction A_V. Line-of-sight stellar motions are modelled by a Gaussian distribution centred at velocity $v_\star$ and with dispersion $\sigma_\star$. Regions around emission lines and bad pixels are excluded from the analysis. SEAGal II describes numerical and other technical aspects of the code.

We apply our synthesis method to the galaxy sample described in the last section. The SDSS spectra cover a wavelength range of 3800–9200 Å, have mean spectral resolution $\lambda/\Delta\lambda \sim 1800$, and were taken with 3-arcsec-diameter fibres. Prior to the spectral fits, the spectra are corrected for Galactic extinction with the maps given by Schlegel, Finkbeiner & Davis (1998) and the extinction law of Cardelli et al. (1989), shifted to the rest frame and resampled from 3400 to 8900 Å in steps of 1 Å.

The result of the procedure is a list of parameters for each galaxy. The most important for discussion in this paper are: (i) the dust-corrected stellar mass inside the fibre; the total stellar mass ($M_\star$) is computed a posteriori after correcting for the fraction of luminosity outside the fibre, assuming that the galaxy $M_\star/L$ does not depend of the radius; (ii) the mean stellar age, weighted either by light, $\langle \log t_\star \rangle_L$, or by mass $\langle \log t_\star \rangle_M$; (iii) the mean stellar metallicity, light and mass-weighted, $\log \langle Z_\star \rangle_L$ and $\log \langle Z_\star \rangle_M$, respectively; (iv) the V-band stellar extinction $A_V^\star$; and (v) the velocity dispersion, $\sigma_\star$. Besides, by subtracting the synthesized spectrum from the observed one, we get a 'pure-emission' residual spectrum, which is useful for analysis of the galaxy emission lines.

2.3 Completeness issues

The volume-limited sample adopted in this work secures a high completeness for galaxies brighter than $M_r \leqslant -19.9$. However, in this work we are also interested in the properties of galaxies divided according to stellar mass; thus, a high completeness in this parameter is needed in order to avoid any bias originating from the sample selection procedure.

We investigate this issue with the help of the mass–luminosity relation of galaxies from a flux-limited sample containing 20 000 objects (hereafter referred to as '20 k sample') selected at random. The total stellar masses are computed after correcting the stellar masses obtained from the spectral synthesis by aperture effects. As for the main sample, this is done by dividing the stellar masses by $(1 - f)$, where f is the fraction of the total galaxy luminosity in a given band outside the fibre. Here, this correction is made by using total and fibre Petrosian magnitudes in the z band.

Fig. 1 shows the mass–luminosity relation for all galaxies in the 20 k sample, and for early- and late-type galaxies distinguished according to the 4000-Å break index measured following the definition given by Balogh et al. (1999) and referred to as $D_n(4000)$. In SEAGal II, we have shown that the optimal value to separate early and late galaxy types is $D_n(4000) = 1.67$. In this figure, we also show the median values (solid lines) and the 10–90 percentiles (dashed lines) of the stellar mass in bins of galaxy luminosity.

In order to select a subsample of galaxies with high completeness in stellar mass, we need to compute the value of $M_\star$ above which it will be complete. Adopting the galaxy luminosity limit for our sample ($M_r \leqslant -19.9$, corresponding to $\log L_r/\mathrm{L}_\odot \geqslant 9.8$, shown in Fig. 1 as the vertical dashed lines), and considering the upper 90 percentile of the distributions for each galaxy type shown in Fig. 1, we found that our galaxy sample will be nearly complete for late-type galaxies with $M_\star \geqslant 1.8 \times 10^{10}\,\mathrm{M}_\odot$, and for early-type galaxies with $M_\star \geqslant 2.8 \times 10^{10}\,\mathrm{M}_\odot$. By using these limits (shown as the horizontal dashed lines in Fig. 1), we then selected a subsample containing 49 453 objects, with a high completeness in stellar mass. Thus, when studying relations involving $M_\star$, we will adopt this subsample in order to avoid any bias introduced by our sample selection procedure. It is convenient to summarize here the samples that will be used in the rest of this paper. In Table 1, we show the basic statistics of the volume-limited and stellar mass-limited samples, and also of a subsample of star-forming galaxies that will be analysed in the next section.

3 THE STAR FORMATION ACTIVITY IN GALAXIES

In this section, we describe some usual tracers of star formation activity in galaxies based on the Hα emission line, and how they are related to spectral synthesis products. Our main intention here is to

Table 1. Summary of the samples adopted in this work.

Sample	Number	Per cent
Volume limited	63 659	100.0
$M_\star$ limited	49 453	77.7
Star-forming galaxies	26 540	41.7

define these quantities and show that the light-weighted mean stellar age behaves as a good tracer of current star formation in galaxies.

3.1 Emission-line related products

The equivalent width (EW) of the Hα emission line is a useful parameter when studying the star formation properties of galaxies. This quantity is related to the ratio between the amount of star formation occurring in a galaxy in the last $\sim 10^7$ yr and its past integrated star formation history. Since the measurement of EW(Hα) does not require flux-calibrated spectra nor intrinsic reddening correction, it has been widely used as an indicator of recent star formation activity in local galaxies, for instance, in works related to the environmental dependence of star formation properties of galaxies (e.g. Lewis et al. 2002; Gómez et al. 2003; Rines et al. 2005).

A more direct and useful tracer of SFR in galaxies is the Hα luminosity (e.g. Kennicutt 1998). When appropriately corrected for underlying absorption and dust extinction, and in the case of fibre-based spectra also for aperture effects, the Hα SFR estimate is found to be consistent with radio, far-infrared, and *u*-band estimates (Hopkins et al. 2003). In our case, the underlying stellar absorption is automatically subtracted when computing the residual spectra (as discussed in Section 2.2). The Hα SFR, corrected by aperture effects, is then simply derived by using the expression adapted from Kennicutt (1998) for a Chabrier initial mass function (0.1–100 $M_\odot$) and with the prescriptions given by Hopkins et al. (2003):

$$\mathrm{SFR_{H\alpha}}(M_\odot\ \mathrm{yr}^{-1}) = 5.22 \times 10^{-42}\, L(\mathrm{H}\alpha)\, 10^{-0.4(r - r_{\mathrm{fibre}})}, \quad (1)$$

where $L(\mathrm{H}\,\alpha)$ is the observed luminosity of Hα (in erg s^{-1}) corrected by nebular extinction with the Hα/Hβ intrinsic intensity ratio, r is the r-band Petrosian magnitude representing the total galaxy flux, and r_{fibre} is the r-band fibre magnitude.[1] Note that since we have corrected the Hα luminosities for extinction with the help of the Hα/Hβ ratio, only galaxies with these two lines measured with a significant S/N will have their SFR(Hα) computed. Consequently, only galaxies with higher levels of star formation activity will have their SFRs evaluated.

Another interesting quantity related to star formation in galaxies is the SFR per unit stellar mass, or specific SFR [SSFR(Hα)], which is associated to the strength of the current burst of star formation relative to the underlying stellar mass of a galaxy (e.g. Guzman et al. 1997). In our case, this parameter is easily obtained by dividing the SFR(Hα) (in $M_\odot$ yr^{-1}) by the dust-corrected stellar mass, $M_\star$.

In order to illustrate the quantities described above, in Fig. 2 we show the relation between EW(Hα) and SFR(Hα), and that between EW(Hα) and the specific Hα SFR. This figure also shows the median values of each relation in bins of r-band galaxy luminosity. It is important to stress here that we only consider galaxies with Hα measured in emission with an S/N greater than 3 (following SEAGal I). In addition, we also restrict this analysis to galaxies with Hα emission coming from normal star-forming regions by excluding hosts of active galactic nuclei (AGN) in the same way as done by SEAGal II. In Fig. 2, we note a clear dependence on galaxy luminosity for the relation between EW(Hα) and SFR(Hα), in the sense that for a given value of EW(Hα), brighter galaxies have higher SFRs. This luminosity dependence disappears when dealing with the specific SFR.

[1] The latter term in this equation is used to correct the SFR estimate by aperture effects by assuming that the Hα luminosity inside the fibre is characteristic of the whole galaxy, and that the continuum flux at the Hα wavelength is well represented by the flux at the effective wavelength of the r-band filter (see details in Hopkins et al. 2003).

3.2 Light-weighted mean stellar age as an indicator of star formation

The mean light-weighted stellar age of a galaxy is related to the formation epoch of massive and bright stars, frequently associated to starbursts. Hence, low values of $\langle \log t_\star \rangle_L$ reflect the recent activity of intense star formation operating in a given galaxy, whereas high values of it indicate that most of the galaxy light comes from older stellar populations, with less-significant, or even none, recent star formation episodes. As this quantity is obtained by our spectral synthesis approach in a robust way, we will inspect its ability in tracing star formation activity of galaxies.

In Fig. 3, we show the relation between $\langle \log t_\star \rangle_L$ and the parameters discussed previously: EW(Hα) and SSFR(Hα). We do not show the relation between $\langle \log t_\star \rangle_L$ and SFR(Hα) since this latter parameter has a dependence on galaxy luminosity, related to the amount of stellar mass recently formed in a galaxy. As in Fig. 2, these relations are also shown in bins of galaxy luminosity [i.e. it is an *extensive* quantity, whereas $\langle \log t_\star \rangle_L$, EW(H$\alpha$) and SSFR(H$\alpha$) are all *intensive* quantities]. We clearly note that this mean stellar age is very sensitive to star formation activity estimated via Hα products. The relations with EW(Hα) and SSFR(Hα) show high Spearman correlation coefficients (-0.58 for both relations). Hence, the $\langle \log t_\star \rangle_L$ figures out as a good tracer of recent star formation activity in galaxies, and since we have measured it for all galaxies in our sample (unlike Hα-based indicators) it is well suited for analysis involving the whole galaxy population, even for galaxies without emission lines.

4 THE ENVIRONMENT

In this work, we use a conventional approach to dealing with galaxy environment. We adopt a non-parametric method to determine the local number density of galaxies, based on the kth nearest neighbour density estimator (kNN; see e.g. Fukunaga 1990 for a statistical description of such an approach). This method fixes a value for k and lets the volume $V(r)$, centred on a given object and extending to its kth nearest neighbour, be a random variable. This volume is large in low-density regions and small in high-density regions. In this way, this method provides a spatial description of the density field, which has been recently explored by Mateus & Sodré (2004) in a study of field galaxies.

When one goes to denser environments, velocity dispersion is high and neglecting peculiar velocities in distance estimates could underrate local densities determined with the kNN method. In order to avoid this effect, a better way to derive local galaxy density via nearest neighbours is by considering a projected distribution of galaxies, instead of a spatial one. This procedure has been intensively used in studies devoted to galaxy environments, since the classical work by Dressler (1980) to more recent works based on Two-degree Field Galaxy Redshift Survey (2dFGRS) (e.g. Lewis et al. 2002) and SDSS (e.g. Gómez et al. 2003) data.

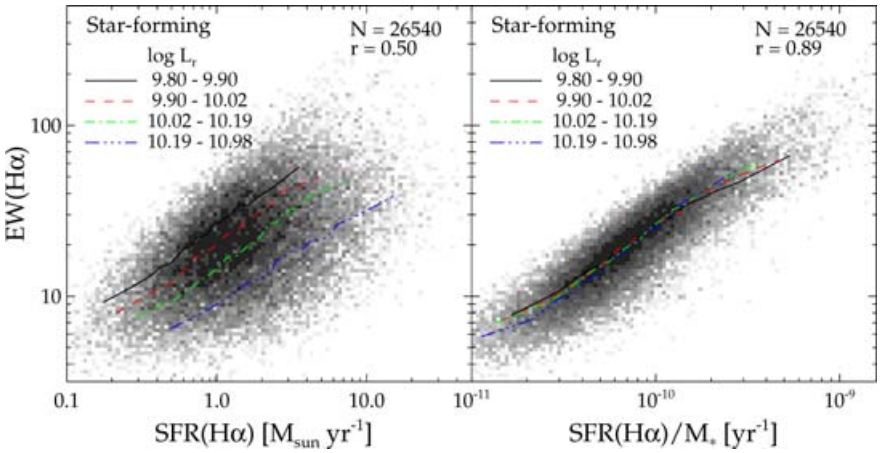

Figure 2. Relations among the tracers of star formation activity based on the Hα emission line. Median values of EW(Hα) as a function of SFR(Hα) (left-hand panel) and SSFR(Hα) (right-hand panel) are shown in bins of *r*-band galaxy luminosity chosen to contain the same number of objects. In this and in the following figures, the median values for each luminosity bin are shown as different lines. The legend in the top left-hand corner shows the range of each bin in which the median values have been evaluated. The numbers at the top right-hand corner are the count of galaxies in each panel and the Spearman correlation coefficient.

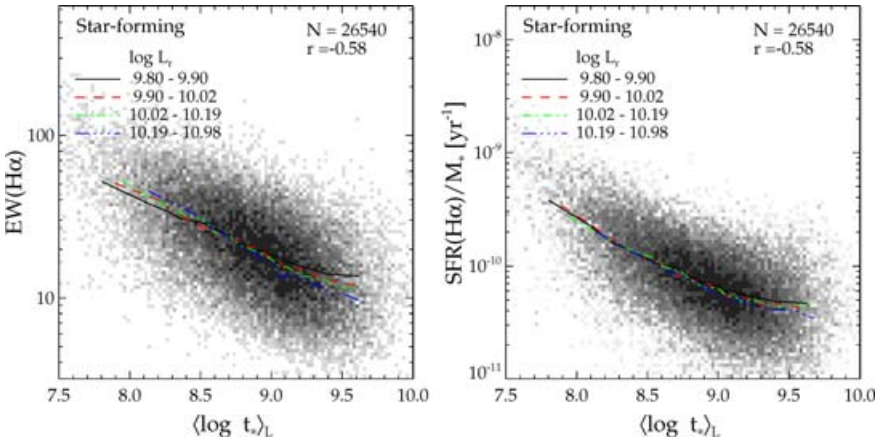

Figure 3. Median values of EW(Hα) and SSFR(Hα) as a function of light-weighted mean stellar age in bins of galaxy luminosity. The numbers at the top right-hand corner are the count of galaxies in each panel and the Spearman correlation coefficient.

A more common approach when dealing with large redshift survey data is to define a limit in a redshift space around a given galaxy, for instance, in the range ± 1000 km s^{-1}, to find its *k*th nearest neighbour (e.g. Blanton et al. 2003; Goto et al. 2003; Balogh et al. 2004). This limit emulates a three-dimensional description of the density field by excluding galaxies in the foreground/background with an objective criterion. As noted by Cooper et al. (2005), projected density estimates with limits in the line-of-sight velocities between ± 1000 and ± 1500 km s^{-1} are best suited for the description of a broad range of environments.

Here, we use the expression $\Sigma_k = k/\pi r_k^2$ to estimate the local galaxy density,[2] where r_k is the projected distance to the *k*th nearest neighbour of a given galaxy. We adopt the usual limit in redshift space of ± 1000 km s^{-1}. Additionally, in our density estimates, we have prevented an incorrect determination of Σ_k due to border effects by excluding galaxies whose *k*th neighbours have projected distances greater than the distance of the galaxy to the closest border of the survey region or of the sample volume. Note that in the search of neighbours and in the density estimates we have used all galaxies in the volume-limited sample independently of the quality of their spectroscopic data.

We have computed our local galaxy density estimates with the values $k = 5$ and 10 in order to assess the influence of the choice of this parameter on the results presented in this work. However, we have found that none of the results discussed in the following sections depends on the values of the *k* tested here. In the rest of this paper, we will adopt the local galaxy density as evaluated from the distance to the 10th neighbour, Σ_{10}.

We have compared our local density estimates defined by Σ_{10} to a global parameter: the distance to the nearest cluster centre from each galaxy in our sample. We searched for galaxy clusters present in our sample with the help of the C4 Cluster Catalogue (Miller et al. 2005), which contains 748 clusters identified in the spectroscopic sample of the SDSS Data Release 2 (DR2). This catalogue is about 90 per cent complete and 95 per cent pure above $M_{200} = 1 \times 10^{14}\, h^{-1}\, \mathrm{M}_\odot$ and within $0.03 < z < 0.12$, thus covering the redshift range of our sample. Therefore, for each galaxy in our sample we

[2] Note that in statistics, $k - 1$ should replace k in the numerator of the expression for Σ_k in order to achieve an unbiased estimate of local density (Fukunaga 1990).

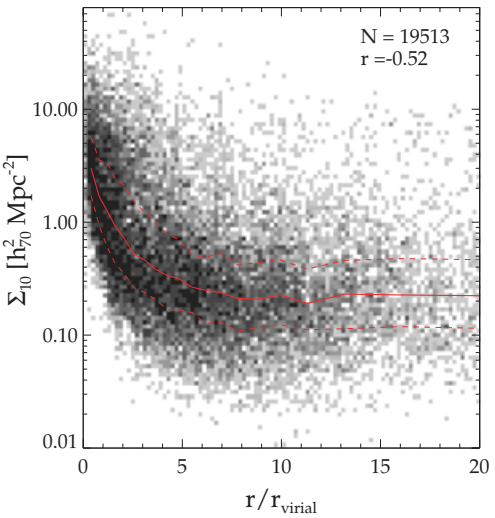

Figure 4. Comparison between local and global definitions of environment. The local galaxy density (Σ_{10}) is plotted as a function of the cluster-centric radius ($r/r_{\rm virial}$). Median values of the relation are shown as the solid line, and their respective quartiles as the dashed lines. In the top right-hand corner are shown the number of galaxies and the Spearman correlation coefficients for the relation.

can compute its distance to the nearest cluster centre, defining in this way a cluster-centric radius normalized by the cluster virial radius. In Fig. 4, we show the relation between our density parameter (Σ_{10}) and the cluster-centric radius ($r/r_{\rm virial}$) only for galaxies located in the regions covered by the DR2 data. There is a clear correlation between the two quantities, mainly for $r/r_{\rm virial} \lesssim 5$, above which we note that the median values of local galaxy density are almost constant.

A possible source of bias in the estimation of local galaxy density in the SDSS data is due to a technical limitation in the procedure of assignment of fibres to spectroscopic targets closer than 55 arcsec in the sky. This problem, referred to as 'fibre collision', becomes very important in denser environments and about 8–9 per cent of selected objects are unobserved for this reason (Stoughton et al. 2002).

In order to assess the significance of this bias in our results, we have searched in the DR4 photometric catalogue for galaxies closer than 55 arcsec of each galaxy in our spectroscopic selected sample, which actually have been rejected in the fibre assignment procedure. Note that these missing galaxies only affect our local galaxy density estimate if they have radial velocities close to those of the selected galaxies. However, as they do not have any redshift information we have overestimated the effects of the fibre collision bias by supposing that all such missing 'neighbours' are at the same redshift as the selected galaxies. From the total of 63 659 selected galaxies in our volume-limited sample, we have found that about 12 per cent of galaxies with missing 'neighbours' are closer than 55 arcsec. We have then evaluated our density estimates by considering that these missing objects were in fact close neighbours. After redoing our analysis with these new densities, we concluded that none of the results shown in this work is affected by the bias due to fibre collision.

5 THE ENVIRONMENTAL DEPENDENCE OF GALAXY PROPERTIES

In this section, we investigate how some physical properties related to the stellar populations of nearby galaxies behave as a function of the local galaxy density. We begin by investigating the dependence of the fraction of galaxies of distinct mean stellar ages and masses on the environment, which can be linked to the classical morphology–density relation. The environmental dependence of star formation activity in galaxies, specially if estimated through the light-weighted mean stellar age parameter, is further investigated. We also analyse how the metallicities of galaxies vary along the density range studied in this work. Finally, the role of stellar mass and luminosity in driving the star formation–density relation is investigated here, mainly through a principal component analysis (PCA) applied to our parameter set.

5.1 Galaxy fractions

It is well established that the fraction of galaxies classified according to distinct morphological types is strongly related to the environment, with high-density regions typical of galaxy clusters being populated essentially by elliptical galaxies, in contrast to the high fraction of spirals found in the field (e.g. Dressler 1980). This galaxy-type segregation is investigated here in terms of two physical galaxy properties: the mean light-weighted stellar age and the stellar mass. SEAGal II studied these parameters in light of the bimodality observed in galaxy populations and found that the mean stellar age of galaxies is primarily responsible for the dichotomy between blue and red galaxies seen in the local Universe (e.g. Strateva et al. 2001; Baldry et al. 2004). They also found that the stellar mass has an additional role in the sense that, blue, star-forming galaxies are preferentially of low mass.

In Fig. 5, we show how the fraction of galaxies in bins of light-weighted mean stellar age (left-hand panels) and stellar mass (right-hand panels) correlates with the local galaxy density. Galaxies are grouped in four bins of $\langle \log t_\star \rangle_L$ and $\log M_\star/{\rm M}_\odot$, each one containing the same number of objects. It is clear from Fig. 5 that high-density environments are populated by galaxies with older stellar populations and larger stellar masses, with the fraction of these objects increasing as the environment becomes denser. The transition in galaxy fractions occurs at a local density of $\Sigma_{10}^t \sim 0.7\, h_{70}^2\,{\rm Mpc}^{-2}$, above which the population of massive galaxies with older stellar populations begins to dominate. This transition density corresponds, on average, to about 2–3 virial radii from cluster centres, as can be deduced from Fig. 4. Additionally, we note that in the case of $M_\star$, the fractions only change for the two extreme bins, whereas intermediate ones possess constant fractions along Σ_{10}. It is worth stressing that the transition shown in Fig. 5 is not the same as the 'break' at a characteristic galaxy density reported by Lewis et al. (2002) and Gómez et al. (2003) that we discuss below, since here we are investigating only galaxy fractions as a function of the local galaxy density, instead of the SFR–density relation itself.

5.2 Star formation activity

Here, we revisit the distribution of the Hα EW as a function of the local galaxy density. In recent years, many works have been devoted to the study of this relation. For instance, Gómez et al. (2003) have investigated the environmental dependence of SFR in galaxies based on the Hα emission line. Their main result was the finding of a break at a characteristic local galaxy density resulting in an abrupt decrease in the EW(Hα) (or SFR) of galaxies in denser regions. Recently, Tanaka et al. (2004) have shown that this break indeed occurs only for fainter galaxies ($M_r^* + 1 < M_r < M_r^* + 2$), with brighter ($M_r < M_r^* + 1$) ones showing EW(H$\alpha$) only monotonically

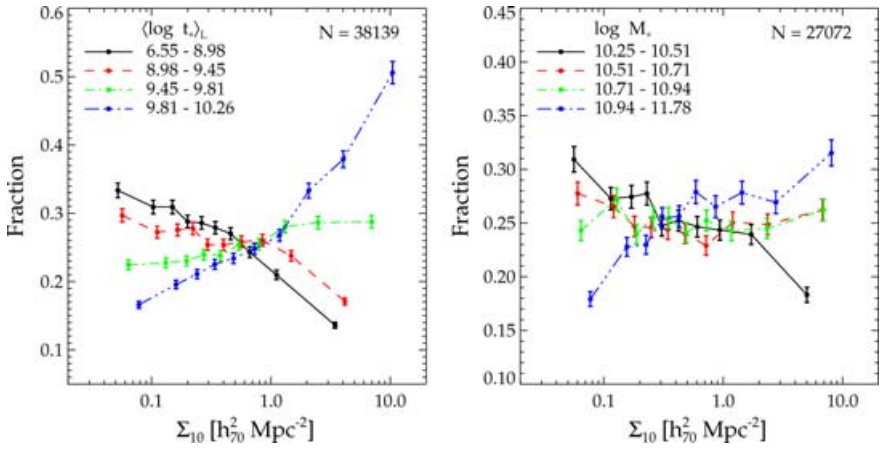

Figure 5. Left-hand panel: the fraction of galaxies in bins of light-weighted mean stellar age (each one containing the same number of galaxies) as a function of the local galaxy density. Right-hand panel: the same, but now for galaxies in bins of dust-corrected stellar mass. The numbers at the top right-hand corner are the count of galaxies in each panel.

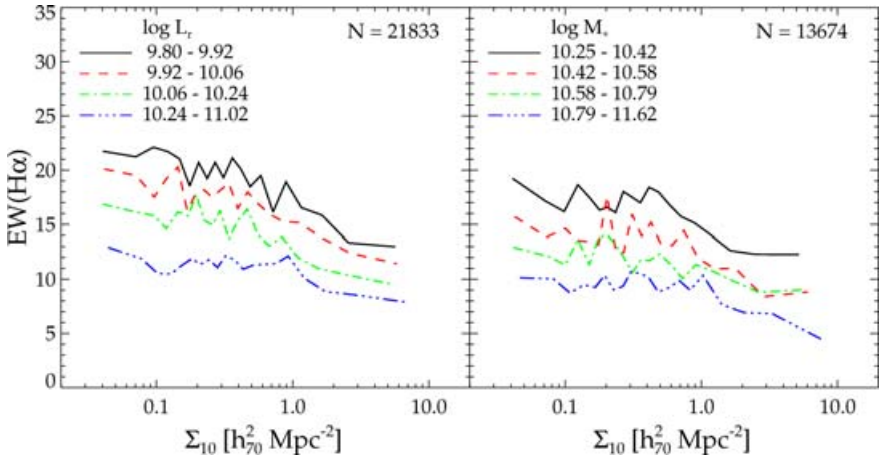

Figure 6. Median values of the Hα EW as a function of local galaxy density, in bins of galaxy luminosity (left-hand panel) and stellar mass (right-hand panel). The numbers at the top right-hand panel are the count of galaxies in each panel.

decreasing with density. Here, we use a more detailed approach to analyse this relation.

In Fig. 6, we present the median values of EW(Hα) as a function of local galaxy density. The median values of EW(Hα) are taken for galaxies grouped in bins of luminosity, $\log L_r/\mathrm{L}_\odot$ (left-hand panel) and stellar mass, $\log M_\star/\mathrm{M}_\odot$ (right-hand panel). In this figure, we show all galaxies with Hα emission line measured with S/N greater than 3, avoiding to include active nucleus hosts (cf. Section 3). This procedure is very robust since the line measurements we have done make it possible to classify a galaxy in detail, as discussed in SEAGal II. Moreover, with the help of spectral synthesis, we can measure only the emission contribution of Hα line, avoiding the inclusion in our analysis of galaxies that would appear with negative values in distributions of EW(Hα) or SFR(Hα), as shown in other works (see e.g. fig. 4 of Gómez et al. 2003).

We note in Fig. 6 that the median values of EW(Hα) for galaxies in all luminosity bins decrease with galaxy density without showing any break (even if we consider all quartiles of the distribution), confirming the result found by Tanaka et al. (2004) for brighter galaxies (our sample contains galaxies with $M_r < M_r^\star + 1.5$). In this sense, the relation between star formation activity and local galaxy density for bright galaxies is independent of galaxy luminosity, since it exists in all bins of $\log L_r/\mathrm{L}_\odot$. This trend is also seen in the right-hand panel of Fig. 6, where galaxies are now divided according to their stellar masses. The absence of a break in Fig. 6 indicates that the relation between star formation activity and local galaxy density decreases monotonically over a wide range of environments, as suggested by Mateus & Sodré (2004).

We also investigate this issue by analysing the environmental dependence of the star formation activity of galaxies spectrally classified as star forming, following the same definition as used in SEAGal II. These galaxies have low stellar masses (about 83 per cent of them have $\log M_\star/\mathrm{M}_\odot < 10.67$) and young mean stellar ages (more than 95 per cent of them have $\langle \log t_\star \rangle_L < 9.53$). In Fig. 7, we show the specific SFR [SSFR(Hα)] as a function of the local galaxy density only for the spectral class of star-forming galaxies. As in Fig. 6, galaxies are divided in bins of luminosity (left-hand panel) and stellar mass (right-hand panel). We note in Fig. 7 that the median values of SSFR(Hα) for star-forming galaxies have almost constant values along the density bins covered by our sample, implying that the specific SFR of star-forming galaxies does not depend on the local galaxy density, confirming the results found by other investigators (e.g. Balogh et al. 2004; Rines et al. 2005).

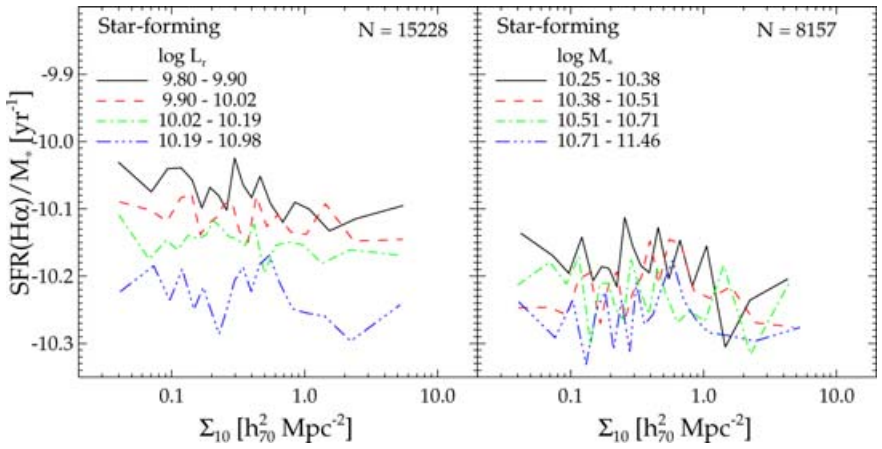

Figure 7. Median values of the specific SFR related to the Hα emission luminosity as a function of local galaxy density, in bins of galaxy luminosity (left-hand panel) and stellar mass (right-hand panel), only for galaxies classified as star forming. The numbers at the top right-hand corner are the count of galaxies in each panel.

5.2.1 Mean stellar ages

An important issue concerning the use of star formation tracers based on emission-line measurements – like those related to the Hα emission line – is the absence of data for galaxies with little (or even none) recent star formation activity, since the emission lines (if they exist) in the spectra of these systems are too weak to be measured with appreciable S/N. Additionally, in galaxies where a starburst is obscured by the presence of huge amounts of dust, the emission lines will also become very weak to be detected. Thus, results from environmental studies based solely on the EW(Hα) or SFR(Hα) parameters could suffer from this kind of bias. In Section 3, we have shown that the mean light-weighted stellar age obtained by spectral synthesis has a good correlation with both EW(Hα) and SSFR(Hα), implying that this parameter is well related to the star formation history of galaxies. In fact, low values of $\langle \log t_\star \rangle_L$ reflect an intense activity of star formation occurring in a galaxy, whereas high values of it are associated to most of the galaxy light coming from older stellar populations. As we measured this parameter for all galaxies in our sample, it is interesting to investigate its dependence on the environment defined by the local galaxy density.

In Fig. 8, we show the mean stellar age weighted by light as a function of the local galaxy density. The median values of $\langle \log t_\star \rangle_L$ are taken for galaxies grouped in bins of luminosity and stellar mass. The behaviour of the mean ages of the stellar populations is distinct when we split galaxies according to L_r or $M_\star$. In order to clarify these trends in terms of the bimodal character of the galaxy populations, we also show in this figure, as the horizontal dashed lines, the value of $\langle \log t_\star \rangle_L$ which better separates early and late galaxy types (see SEAGal II for details).

We note in the left-hand panel of Fig. 8, that the median values of $\langle \log t_\star \rangle_L$ increase significantly as the environment becomes denser, independently of the galaxy luminosity, with the relation for fainter galaxies being steeper than that of brighter ones. The properties of the population of fainter galaxies also tend to change at $\Sigma_{10} \lesssim 5h_{70}^2$ Mpc^{-2}, where the median values of $\langle \log t_\star \rangle_L$ cross the dividing line which distinguishes galaxies dominated by young stellar populations (late types) and galaxies with older stars (early types). On the other hand, the mean stellar ages of galaxies with different stellar masses (seen in the right-hand panel of Fig. 8) behave in a distinct way with respect to the local galaxy density. Low-mass galaxies have median values of mean stellar ages slightly varying along the bins of

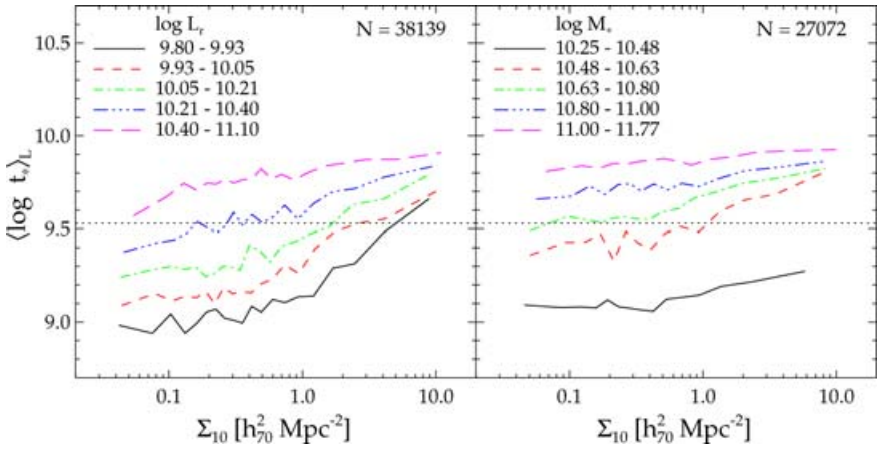

Figure 8. Median values of the mean stellar age weighted by light as a function of the local galaxy density, in bins of galaxy luminosity (left-hand panel) and stellar mass (right-hand panel). The horizontal dashed lines correspond to the optimal value of $\langle \log t_\star \rangle_L$ to split galaxies between early and late types. The numbers at the top right-hand corner are the count of galaxies in each panel.

density, showing low values of $\langle \log t_\star \rangle_L$ – characteristic of late-type galaxies – in all environments. However, this behaviour for the lowest stellar mass bin may be affected by incompleteness due to the low fraction of early-type galaxies selected in the range $10.25 < \log M_\star < 10.48$. The most-massive galaxies also show a slight change in the median values of $\langle \log t_\star \rangle_L$ as galaxy density increases, but their values are higher everywhere. The steeper relation is seen for galaxies with intermediate stellar masses ($\sim$3–6 $\times$ 10^{10} $M_\odot$), which shows a transition from late to early galaxy types at $\Sigma_{10} \sim 0.3$–$1.0\ h_{70}^2$ Mpc^{-2}.

Therefore, an age–density relation is clearly obtained when galaxies are divided according to their luminosities. However, the relation is not so evident when they are grouped in bins of stellar mass. This indicates that the galaxy luminosity and stellar mass could be playing distinct roles in driving the age–density relation shown in this work. We will appropriately address this question in Section 5.4.

5.3 Stellar metallicities

We now investigate the environmental dependence of another important physical parameter of galaxies, the mean stellar metallicity. In Fig. 9, we plot $\log \langle Z_\star \rangle_L$ and $\log \langle Z_\star \rangle_M$ versus local galaxy density, for galaxies in bins of luminosity (left-hand panels) and stellar mass (right-hand panels). The relation between $\log \langle Z_\star \rangle_L$ and local density becomes less steep as galaxy luminosity increases. The result of this trend is that fainter galaxies in low-density regions have subsolar metallicities, whereas in denser regions they have high metallicities similar to that of the brightest galaxies in our sample. For galaxies divided according to stellar mass, the trends are similar. The stellar metallicity of low-mass galaxies increases as the environment becomes denser, while massive galaxies have almost constant values of $\log \langle Z_\star \rangle_L$ along density bins. In the case of the mass-weighted mean stellar metallicity ($\log \langle Z_\star \rangle_M$) versus local galaxy density, the trends are similar, although less steep than those for $\log \langle Z_\star \rangle_L$. The main difference is that luminous (massive) galaxies also tend to have more metallic stellar populations in denser environments, as shown in the bottom panels of Fig. 9.

It is interesting to note that the values of $\log \langle Z_\star \rangle_L$ are related to mean metallicities of the stellar populations which contribute significantly to galaxy light. Thus, one could expect that they are directly associated to recent episodes of star formation in galaxies. In this way, low-mass (or fainter) galaxies in denser environments, which are currently forming stars (following the results from Fig. 8), tend to have more metal-rich stellar populations than their counterparts in regions of lower densities. Low-mass galaxies have substantial amounts of gas to keep their high SFRs. This gas could have been pre-enriched earlier preferentially in high-density environments, where the star formation activity was higher in the past (e.g. Madau, Ferrara & Rees 2001; Scannapieco, Ferrara & Madau 2002). Thus, one explanation is that these galaxies have already been formed in that denser environment, but have not stopped to form stars until the present epoch. Thus, this result is additionally supported by the observed 'downsizing' in galaxy formation (e.g. Cowie et al. 1996; Kodama et al. 2004; Juneau et al. 2005, among others), where

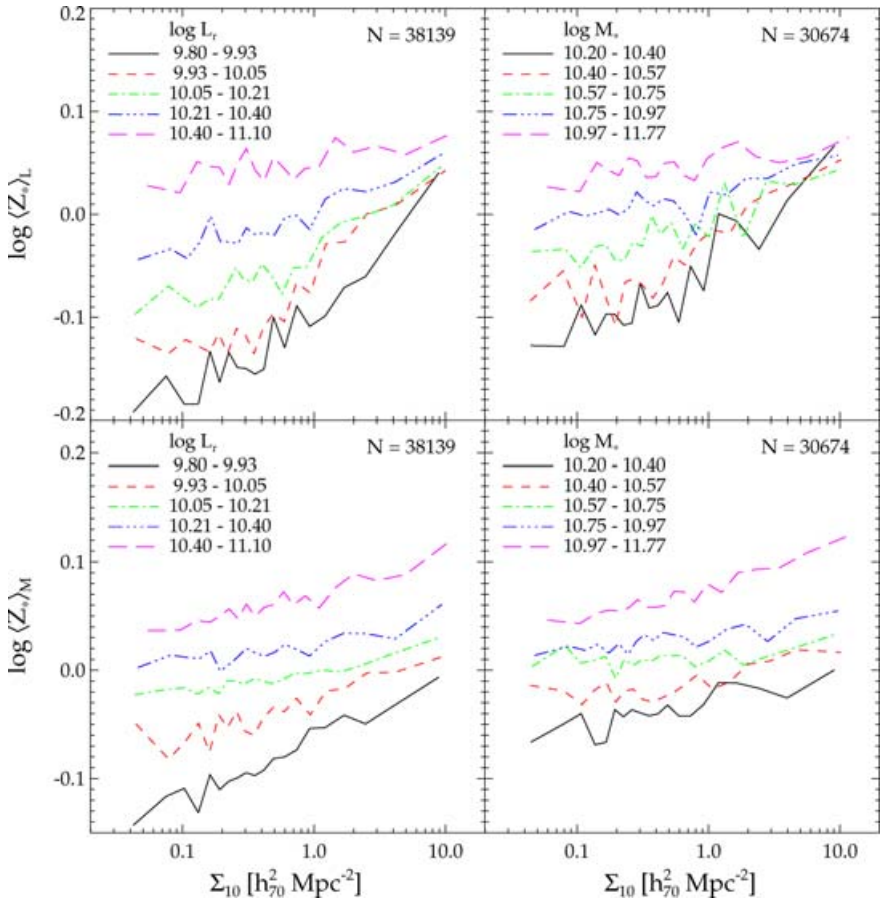

Figure 9. Median values of light-weighted stellar metallicity as a function of local galaxy density for galaxies in bins of luminosity (left-hand panel) and stellar mass (right-hand panel). The numbers at the top right-hand corner are the count of galaxies in each panel.

massive galaxies have formed most of their stellar masses at early times. However, the processes that have kept the continuous star formation in those low-mass galaxies are not well understood.

5.4 The role of stellar mass and luminosity

The relation between the mean stellar age of galaxies and their environment (defined by the local galaxy density) shows that galaxy luminosity and stellar mass play distinct roles in defining the environmental dependence of star formation properties of galaxies. In general, that dependence exists independently of L and only for an intermediate stellar mass range characterized by a transition in galaxy properties.

Another way to visualize these trends is shown in Figs 10 and 11, where we show the distributions of $\langle \log t_\star \rangle_L$ for galaxies in vertical bins of local galaxy density, and horizontal bins of stellar mass (Fig. 10) and luminosity (Fig. 11). Each bin in stellar mass (or luminosity) has been built to have the same number of objects, whereas the bins in $\log\ \Sigma_{10}$ are equally spaced. From the comparison of these figures, we note that the age distributions are distinct when galaxies are divided according to stellar mass or luminosity, mainly for objects in the extreme bins. In denser environments (corresponding to $0.91 < \log \Sigma_{10} < 1.86$), less-luminous galaxies have a $\langle \log t_\star \rangle_L$ distribution peaked at older ages, whereas in low-density regions the distribution is double-peaked, unveiling the bimodal character of the galaxy population. On the other hand, in the case of galaxies divided according to stellar mass, the $\langle \log t_\star \rangle_L$ distribution for low-mass galaxies in denser environments is broader, without showing any peak. As local density decreases, the distributions are peaked at younger ages, indicative of the dominance of low-mass star-forming galaxies in low-density environments. At the other extreme, represented by very luminous and massive galaxies, the distributions are similar, with the only difference being due to a larger fraction of galaxies with low values of $\langle \log t_\star \rangle_L$ in the distributions for luminous galaxies. It is also interesting to note the differences in the distributions for two extreme environments. In denser regions, galaxies divided by luminosity show a conspicuous peak centred at older ages in all bins considered in Fig. 11. On the other hand, for galaxies divided by stellar mass there is a growth of the peak at $\langle \log t_\star \rangle_L > 9.5$ from the low-mass to the most-massive bin shown in Fig. 10. However, note that for the lowest stellar mass bin the absence of older early-type galaxies may be a reflex of our sample selection procedure to overcome the stellar mass incompleteness in our sample (Section 2.3).

We also investigate the environmental dependence of a combination of stellar mass and luminosity parameters, namely the $M_\star/L$ of galaxies in our sample as inferred by spectral synthesis. In Fig. 12, we show the relation between the galaxy $M_\star/L$ (in r band) and local density in different bins of r-band galaxy luminosity for (a) all galaxies in our sample, (b) early-type galaxies with $D_n(4000) > 1.67$ and (c) late-type galaxies with $D_n(4000) < 1.67$. We note that, at fixed luminosity, galaxies inhabiting high-density environments tend to be more massive than their counterparts in regions of low density; the $M_\star/L_r$ ratio of these objects increases by 40–50 per cent from low- to high-density regions. The relation is also steeper for the faintest bin shown in the plot. Additionally, the relations for early- and late-type galaxies taken individually are independent of local galaxy density, implying that the increasing of

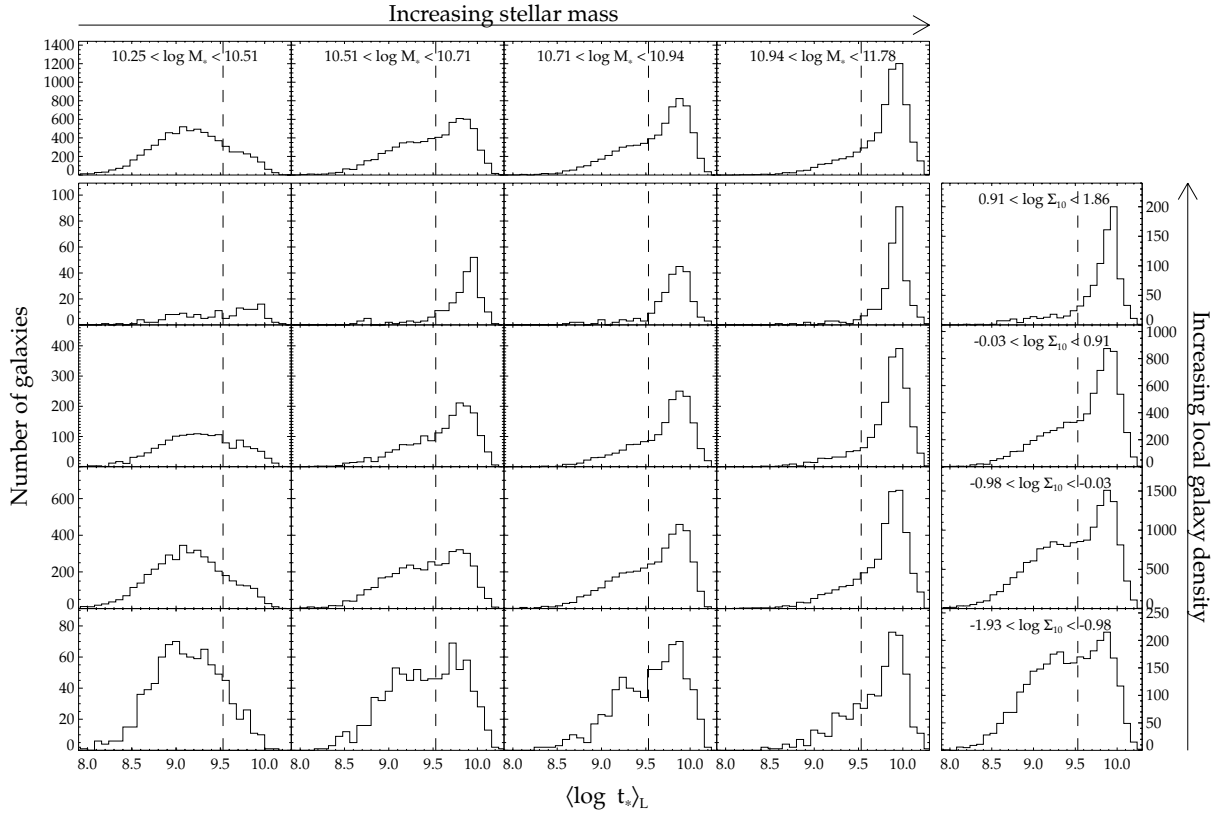

Figure 10. Distributions of mean light-weighted stellar ages for galaxies in bins of local galaxy density and stellar mass. The dotted lines in each panel are the age value used to distinguish early and late galaxy types. The range for each bin, as well as the cumulative distributions, is shown in the top panels, for stellar mass, and in the right-hand panels, for local galaxy density.

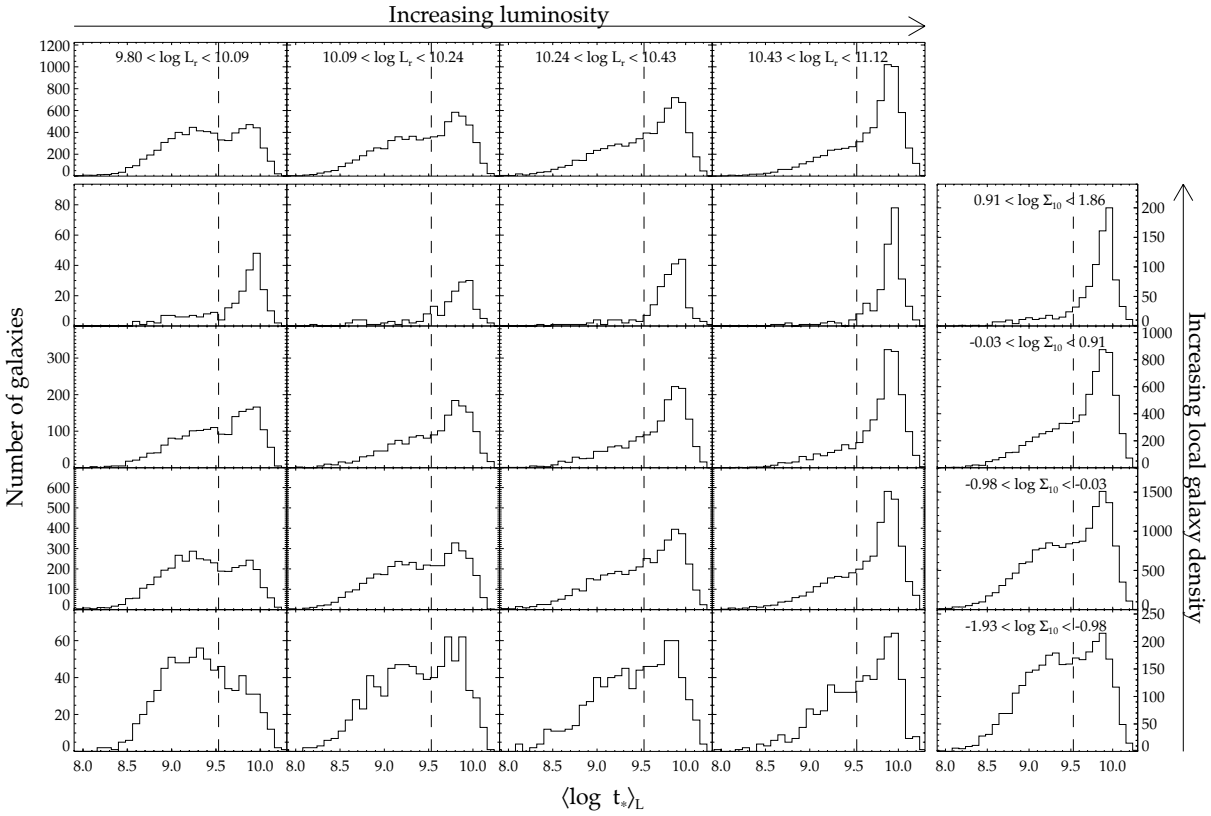

Figure 11. The same as Fig. 10, but in bins of luminosity, instead of stellar mass.

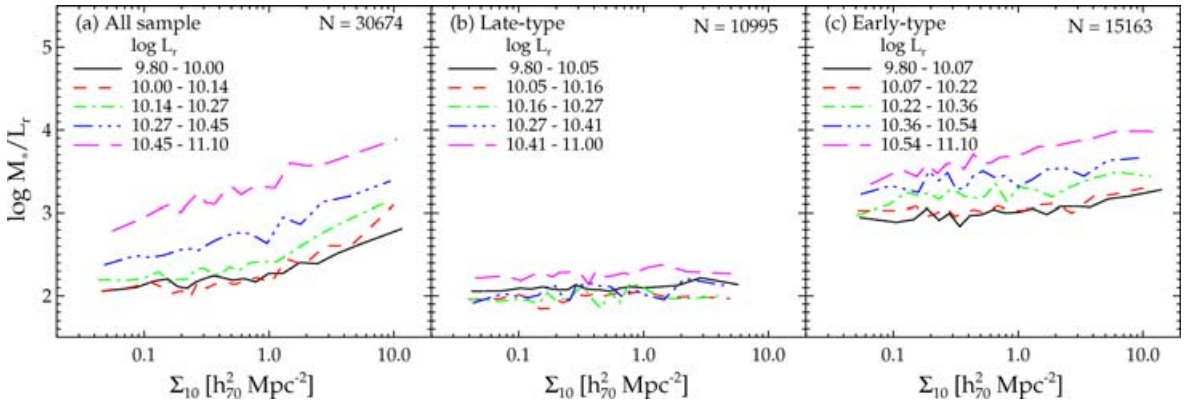

Figure 12. Median values of the $M_\star/L$ as a function of local galaxy density for galaxies in bins of luminosity. The plot in (a) is for all galaxies in our sample, (b) for early-type galaxies with $D_n(4000) > 1.67$ and (c) for late-type galaxies with $D_n(4000) < 1.67$. The numbers at the top right-hand corner are the count of galaxies in each panel.

$M_\star/L_r$ as the environment becomes denser is related to the prevalence of massive systems in high-density regions, as shown in Fig. 5. Only for the most-luminous galaxies there is an increment of $M_\star/L_r$ as a function of local density.

5.5 Principal component analysis

In the previous sections, we have investigated the environmental dependence of the mean light-weighted stellar age, stellar mass, stellar metallicity and $M_\star/L$ in order to understand how galaxy properties are related to the environment. Here, we will investigate this issue through a different approach, based on a useful statistical technique frequently adopted to finding patterns in high-dimensional data.

The parameter set discussed in this section was examined in more detail by means of a PCA in order to determine the combinations of parameters which summarize the distribution of the whole set. PCA is able to identify patterns in a data set and express the data in such a way as to highlight their similarities and differences. This technique is particularly useful for reducing the dimensionality of a data space by identifying the linear combinations of input parameters with maximum variance, called 'principal components' (Murtagh & Heck 1987; Sodre & Cuevas 1997).

A PCA was carried out on the combination of the parameter set $\{\langle\log t_\star\rangle_L, \log M_\star, \log \Sigma_{10}, \log L_r, \log M_\star/L_r\}$ to determine the variables that account for the large amount of variance and hence provide a useful description of the environmental dependence of galaxy properties. We have followed the same procedure as used in the previous sections by dividing the galaxy sample in bins of luminosity and stellar mass containing the same number of objects. A PCA was then executed for each bin separately.

We found that the principal component of highest variance (PC1) accounts for more than 90 per cent of the total variance for all bins considered. The remaining variance is mainly accounted for the second principal component (PC2). Although each principal component is a linear combination of all the input variables, it is interesting to verify whether some variables in the parameter set are well correlated with the main components because, in this case, they are responsible for a significant fraction of the sample variance. In Table 2, we show the Spearman rank correlation coefficients between the two principal components and the five parameters in our input set, for each bin divided by luminosity and stellar mass. We found that the local galaxy density ($\log \Sigma_{10}$) shows the strongest relation with the PC1; the Spearman rank correlation coefficient between this parameter and the PC1 is almost unity. Moreover, the PC2 shows a significant correlation with the $\langle\log t_\star\rangle_L$, with correlation coefficient greater than 0.9. Thus, the PC1–PC2 plane is well represented by the age–density relation in all bins of luminosity and stellar mass investigated here.

Additionally, to verify the behaviour of the other parameters we are investigating, we have excluded the mean stellar age from the input set. The PCA was then carried out on the parameter set $\{\log M_\star, \log \Sigma_{10}, \log L_r, M_\star/L_r\}$. For this set, the results indicate that the PC1 alone explains more than 95 per cent of the sample variance for bins divided by luminosity and stellar mass. The PC2 is responsible for almost all the remaining variance. The Spearman rank correlation coefficients among these two principal components and the parameters in the input set are shown in Table 3 for each bin divided by luminosity and stellar mass. We found that the local galaxy density is again well correlated with the PC1 ($r_S = 1$). The PC2 correlates well with both $M_\star$ and $M_\star/L_r$ for bins in L_r and with $\log L_r$ and $M_\star/L_r$ for bins in $M_\star$.

These results give clear evidence of the SFR–density relation present in our data since the local galaxy density is primarily responsible for the largest amount of sample variance and the mean light-weighted stellar age of galaxies is the secondary source of that variance. Moreover, we note that galaxy luminosity does not have any significant correlation with the principal components, whereas stellar mass and $M_\star/L$ can be considered as the drivers of the sample variance if one excludes the SFR–density relation.

Table 2. Spearman rank correlation coefficients for the five-parameter set.

	$\langle\log t_\star\rangle_L$	$\log M_\star$	$\log\ \Sigma_{10}$	$\log L_r$	$M_\star/L_r$
		$9.80 < \log L_r < 9.96$			
PC1	0.28	0.23	0.99	−0.01	0.24
PC2	−0.96	−0.81	−0.10	−0.10	−0.82
		$9.96 < \log L_r < 10.13$			
PC1	0.28	0.22	1.00	−0.01	0.23
PC2	−0.96	−0.78	−0.12	−0.11	−0.80
		$10.13 < \log L_r < 10.34$			
PC1	0.23	0.18	1.00	0.03	0.19
PC2	−0.97	−0.72	−0.10	−0.15	−0.75
		$10.34 < \log L_r < 11.10$			
PC1	0.20	0.18	1.00	0.09	0.19
PC2	−0.95	−0.68	−0.11	−0.35	−0.70
		$10.25 < \log M_\star < 10.51$			
PC1	0.16	0.08	1.00	−0.10	0.14
PC2	−0.99	−0.35	−0.07	0.36	−0.55
		$10.51 < \log M_\star < 10.71$			
PC1	0.24	−0.01	1.00	−0.17	0.17
PC2	−0.97	−0.08	−0.09	0.47	−0.53
		$10.71 < \log M_\star < 10.94$			
PC1	0.17	0.02	1.00	−0.08	0.11
PC2	−0.98	−0.09	−0.07	0.39	−0.50
		$10.94 < \log M_\star < 11.78$			
PC1	0.15	0.09	1.00	0.04	0.10
PC2	−0.98	−0.29	−0.07	−0.04	−0.41

Table 3. Spearman rank correlation coefficients for the five-parameter set excluding the mean stellar age.

	$\log M_\star$	$\log \Sigma_{10}$	$\log L_r$	$M_\star/L_r$
		$9.80 < \log L_r < 9.96$		
PC1	0.19	1.00	−0.01	0.20
PC2	−0.98	−0.09	−0.20	−0.98
		$9.96 < \log L_r < 10.13$		
PC1	0.18	1.00	−0.02	0.20
PC2	−0.98	−0.09	−0.22	−0.98
		$10.13 < \log L_r < 10.34$		
PC1	0.15	1.00	0.03	0.16
PC2	−0.98	−0.08	−0.32	−0.96
		$10.34 < \log L_r < 11.10$		
PC1	0.17	1.00	0.09	0.18
PC2	−0.99	−0.10	−0.79	−0.69
		$10.15 < \log M_\star < 10.46$		
PC1	0.07	1.00	−0.10	0.14
PC2	−0.24	−0.08	0.87	−0.96
		$10.46 < \log M_\star < 10.67$		
PC1	−0.00	1.00	−0.16	0.16
PC2	0.11	−0.09	0.96	−0.95
		$10.67 < \log M_\star < 10.91$		
PC1	0.03	1.00	−0.08	0.11
PC2	0.27	−0.05	0.97	−0.90
		$10.91 < \log M_\star < 11.78$		
PC1	0.10	1.00	0.04	0.10
PC2	−0.92	−0.03	−0.95	0.07

6 DISCUSSION

6.1 Overview

We have investigated the environmental dependence of some stellar population properties of galaxies in order to advance in our current understanding about the evolution of galaxies in distinct environments. The most intriguing result shown here is that the relations between local galaxy density and properties related to star formation is distinct when we split galaxies in bins of luminosity or stellar mass.

The results shown in the last section will be inspected here in light of two evolutionary paths by which galaxies can evolve. In the first one, galaxy properties (mainly related to star formation and gas properties) are affected by environment through well-known physical mechanisms acting on galaxies. This path, linked directly to the environment, gives origin to a *nurture* perspective for galaxy

evolution. The second path is related to the initial conditions established during galaxy formation, which could account for the relations between galaxy properties and environment. Thus, it is related to a *nature* perspective driving galaxy evolution.

6.2 The star formation–density relation: a nurture perspective?

Recent galaxy redshift surveys have improved our understanding about what is happening with the star formation in galaxies inhabiting different environments. Works carried out by Lewis et al. (2002) using the 2dFGRS data, and by Gómez et al. (2003) using the EDR SDSS data, have revealed a characteristic density at $\sim$1 h_{75}^2 Mpc^{-2} (corresponding to a cluster-centric radius of 3–4 virial radii) associated to a 'break' in the SFR–density relation. Below this density the SFR increases only slightly, whereas at denser regions it is strongly suppressed. Tanaka et al. (2004) have complemented these studies by finding that the break in the SFR–density relation is seen only for fainter galaxies ($M_r^* + 1 < M_r < M_r^* + 2$), while the relation for brighter galaxies ($M_r < M_r^* + 1$) shows no break. Various physical mechanisms are advocated to explain these trends, but in general it is supposed that star formation properties of bright galaxies are affected by low-velocity interactions, while those of faint galaxies are affected by starvation (or strangulation).

In this work, we have investigated relatively bright objects ($M_r \leqslant M_r^* + 1.5$) and for a set of galaxies with Hα line in emission we have found no break or characteristic density in the relation between EW(Hα) and local galaxy density, independently of galaxy luminosity (see Fig. 6). Apparently, this result is in conflict with the conclusions reached by Lewis et al. (2002), Gómez et al. (2003) and Tanaka et al. (2004) that the star formation properties of (faint) galaxies change abruptly when one goes to denser environments. Here, we clarify this question by investigating the colour–density relation for galaxies in our sample. For comparison purposes, this procedure is similar to that done by Tanaka et al. (2004) and shown in their fig. 2. It is worth stressing that galaxy colours are measured in an uniform way by the SDSS photometric pipeline, that is, they do not depend on the methodology employed to compute them. In addition, the colour–density relation, as discussed by Tanaka et al. (2004), is very similar to the EW(Hα)–density relation.

We show in Fig. 13 the relation between the $(g - i)$ colour and the local galaxy density for galaxies divided in two bins of r-band luminosity. In the left-hand panel, we show the relation for all galaxies in our sample. A clear break is seen at $\Sigma_{10} \sim 1\ h_{70}^2$ Mpc^{-2} in the relation for faint galaxies, in complete agreement with the results discussed by Tanaka et al. (2004). On the other hand, bright galaxies tend to become redder in dense environments following a monotonically increasing relation. In the right-hand panel of Fig. 13, we show the same relation but now restricting the sample to a set of galaxies with Hα detected in emission (avoiding to include AGN hosts, as discussed in Section 3). In this case, galaxies also tend to become redder in denser environments, but without showing any break at a characteristic density, even for faint galaxies. Thus, from the inspection of Fig. 13 we conclude that the break seen in the colour–density relation, or in the SFR–density relation discussed by Gómez et al. (2003), is associated to the reduced fraction of star-forming galaxies in denser environments, as discussed in Section 5.1, confirming the results shown by Balogh et al. (2004). Thus, in Gómez et al. (2003) and Tanaka et al. (2004), for instance, the inclusion of absorption-line dominated galaxies (those with negative EW values) originated the break in the star formation–density relation at a particular local density, which actually is related to an environment where the fraction of galaxies without recent star formation activity begins to dominate.

These results also indicate that the decrease in the fraction of star-forming galaxies in dense environments occurs in a wide range of densities. A similar conclusion was reached by Mateus & Sodré (2004) in a study on the environmental dependence of the fraction of star-forming and passive galaxies in a sample of field galaxies drawn from the 2dFGRS data. Even in rarefied environments, the fraction of star-forming galaxies decreases significantly with increasing local galaxy density. Thus, there is a general consensus that physical mechanisms suppressing star formation in galaxies are not inherent only to the densest environments related to galaxy clusters. It is also interesting to note that faint and bright galaxies seem to have evolved through distinct evolutionary paths, and different physical mechanisms could be at work.

However, the relevance of such mechanisms acting on galaxies today may be important only in some particular cases. Balogh et al. (2004) have confirmed this trend by combining samples from the 2dFGRS and SDSS, with emphasis on environments related to galaxy groups. These authors argued that galaxies in dense regions have had typically more interactions than those in low-density regions over a longer period of time. Thus, it seems that galaxy transformations induced by environment have taken place more effectively at higher redshifts. In fact, Kauffmann et al. (2004) have

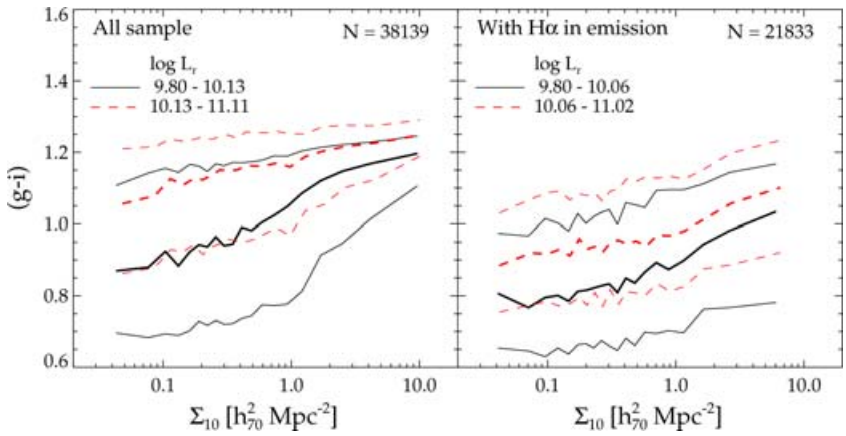

Figure 13. Left-hand panel: median values (thick lines) and respective quartiles (thin lines) of $(g - i)$ colour as a function of local galaxy density for all galaxies in our sample divided in two bins of galaxy luminosity. Right-hand panel: the same, but now restricted only to galaxies with Hα detected in emission. The numbers at the top right-hand corner are the count of galaxies in each panel.

demonstrated that relations between structural parameters and stellar mass have little dependence on local galaxy density, indicating that these relations were already established at early times. In this way, mechanisms that are effective in disturbing the structure of galaxies (affecting the concentration index and surface mass density) are not favoured by these results.

6.3 A natural path for galaxy evolution

In the last section, we have shown that the nurture hypothesis which is invoked to explain galaxy evolution in distinct environments also explains the observed star formation–density relation in the local Universe. Indeed, in the hierarchical scenario of galaxy formation, as galaxy clustering evolves, the density around a galaxy tends to increase in all environments. Higher density probably means more interactions which could, in principle, play a significant role in originating the relation between star formation activity in galaxies and local galaxy density.

The first numerical simulations with CDM initial conditions (e.g. Frenk et al. 1985, 1988) already suggested that the morphology–density relation is a natural product of hierarchical clustering. The high-redshift progenitors of today cluster galaxies were formed in high-density regions, which tend to collapse earlier than low-density environments (Kaiser 1984; Davis et al. 1985; Bardeen et al. 1986). Galaxies formed in high-density regions tend to be ellipticals, because discs are destroyed by frequent interactions and the hot gas does not cool enough to form new stars. Thus, it is expected that the oldest galaxies were formed earlier and preferentially in high-density regions; galaxies in low-density environments are able to keep their cold gas and form stars. Consequently, a natural path for galaxy evolution emerges, with galaxies in denser environments being more evolved than those in low-density regions (Benson et al. 2001).

Recently, Juneau et al. (2005), using a sample of high-redshift galaxies from the Gemini Deep Deep Survey (GDDS), investigated the star formation history of galaxies and its dependence on stellar mass. They showed that the most-massive galaxies formed most of their stars earlier than intermediate- and low-mass galaxies. This trend gives support to an apparent anti-hierarchical behaviour, commonly referred to as 'downsizing' in galaxy formation (e.g. Cowie et al. 1996; Kodama et al. 2004). This picture, where massive galaxies stopped star formation at early times, whereas most low-mass systems continue to form stars actively, is supported by the analysis of galaxies in the local Universe (Kauffmann et al. 2003; Heavens et al. 2004; SEAGal II), as well as by the observation of a large population of massive galaxies at high redshift (e.g. Chen & Marzke 2004; Glazebrook et al. 2004, among others).

These trends have been recovered by recent high-resolution simulations (e.g. Weinberg et al. 2004) and semi-analytic models of galaxy formation (e.g. Menci et al. 2005; de Lucia et al. 2006). On the observational side, the discovery of an overdensity of galaxies (or protocluster) at $z = 2.3$ by Steidel et al. (2005), with a significant fraction of old galaxies, is consistent with the theoretical expectation for the acceleration of structure formation in denser regions. This is in agreement with the conclusions drawn by Einasto et al. (2005), that clusters in high-density environments evolve more rapidly than those in low-density regions.

6.4 A nature via nurture scenario

In this work, we have confirmed that high-density environments are dominated by massive galaxies with the oldest stellar populations in the local Universe, which can be associated to the early-type galaxies of the morphology–density relation. We have also found that the recent star formation activity of less-massive galaxies, as inferred by the mean light-weighted age of their stellar populations, does not change significantly along the density range presented in this work. This result suggests that these low-mass galaxies have large amounts of star formation in low- as well as in high-density regions of the local Universe. However, as the lowest stellar mass bin considered in this work is dominated by late-type galaxies, with the fraction of low-mass early-type galaxies being affected by the selection criteria adopted here, this result should be confirmed by other observations. At the other extreme, the most-massive galaxies in our sample have high values of mean stellar age independently of the environment where they are found. In short, massive galaxies have older stellar populations everywhere. Only for an intermediate mass range ($\sim$3–6 $\times$ 10^{10} $M_{\odot}$), associated to the transition in galaxy properties (see e.g. SEAGal II), the recent star formation activity of galaxies appears to decrease with increasing galaxy density. On the other hand, when we take galaxies divided according to their luminosities, instead of stellar masses, the star formation activity of brighter galaxies and of fainter ones decreases significantly when one goes from low- to high-density environments, resulting in the well-known star formation–density relation for galaxies selected by luminosity (e.g. Lewis et al. 2002; Gómez et al. 2003; Balogh et al. 2004; Tanaka et al. 2004; Rines et al. 2005).

We have also shown in Fig. 12 that, on average, galaxies with similar luminosities in high-density environments have higher $M_{\star}/Ls$, that is, they tend to be more massive than their counterparts in regions of low density (see also Tully 2005 for a similar result related to galaxy groups, and Einasto et al. 2005 for galaxy clusters). Thus, the fact that galaxies of all luminosities present star formation activity decreasing with increasing density is related to the higher stellar masses of galaxies in denser environments, independently of their luminosities. Additionally, from recent results concerning the existence of a downsizing in the processes regulating star formation in galaxies, we expect that most-massive galaxies have stopped to form stars at early times, perhaps thanks to internally driven mechanisms such as a mass threshold below which star formation was not successful (Martin & Kennicutt 2001; Jimenez et al. 2005). Thus, the star formation–density relation found for galaxies divided according to their luminosities, being steeper for fainter galaxies (Tanaka et al. 2004), should be a 'natural' consequence of galaxy evolution.

These results are also supported by the recent findings obtained by Tanaka et al. (2005) in a study on the build-up of the colour–magnitude relation of galaxies as a function of the environment. They also confirmed the downsizing way for the evolution of galaxy properties, with the star formation processes being displaced from massive to low-mass galaxies, and from galaxies in denser to low-density environments, as the evolution proceeds. In addition, our work can also be related to the recent study carried out by Poggianti et al. (2006), who have investigated the evolution of the proportion of star-forming galaxies (defined with the EW [O II]) in clusters since $z = 0.4$–0.8 (from a sample obtained with the ESO Distant Cluster Survey) to $0.04 < z < 0.08$ (from an SDSS cluster sample). Poggianti et al. argued that the star formation–density relation should have a 'primordial' component and an 'evolved' one, each of them showing distinct environmental dependencies, and that the relation is established at very high redshift at the moment of formation of the first stars in galaxies. This scenario is particularly linked to the trends shown by our own results.

The trend related to stellar metallicity shown in Fig. 9 reinforces these ideas: low-mass galaxies in denser environments are

metal-rich compared with those in low-density regions. This arises from the fact that denser regions tend to be more evolved than rarefied environments. Thus, low-mass galaxies in dense regions have already been established in such environments, but have not stopped to form stars until the present epoch, contrarily to the evolution of massive systems. In this sense, a natural path for galaxy evolution proceeds via a nurture way mainly at high redshifts: massive galaxies have been formed in denser regions and evolved in an accelerated way, contrasting with a more *unsocial* life of low-mass galaxies preferentially inhabiting low-density regions of the Universe. This is also related to the timing of the process of formation of early-type galaxies that occurred about 1–2 Gyr earlier in cluster environments compared to the field (Thomas et al. 2005; Clemens et al. 2006). In this view, denser environments behave as an accelerator of the galaxy formation process, amplifying small natural differences imprinted on galaxies in their formation epoch. This results that 'nature' necessarily acts *via* 'nurture' effects.

In this 'nature via nurture' scenario for galaxy evolution, the environmental dependence of the star formation properties of galaxies, commonly related to some (or various) physical mechanisms acting on late-type galaxies infalling on to galaxy clusters, is determined by the higher $M_\star/L$ of galaxies in denser environments, in addition to the observed downsizing in galaxy formation. These two ingredients play a crucial role in defining the star formation–density relation observed in luminosity-divided samples. Nevertheless, we note that environmental effects on galaxy properties really take place in some cases, such as the existence of post-starburst galaxies in clusters (e.g. Dressler & Gunn 1983; Dressler et al. 1999; Poggianti et al. 1999; Tran et al. 2003), passive spirals (e.g. Goto et al. 2003), and short starburst galaxies (Balogh et al. 1999; Mateus & Sodré 2004). However, the fraction of such 'environment-product' objects is very reduced, indicative of a very rapid and efficient mechanism acting on these galaxies or actually due to the rarity of such transformations in the nearby Universe.

7 SUMMARY

In this fourth paper of the SEAGal collaboration, we have shed some light on the discussion about the environmental dependence of galaxy properties in the local Universe. We based our analysis on the stellar population properties of galaxies in a volume-limited sample drawn from the SDSS DR4. The application of a spectral synthesis method to the data produces robust estimators for mean stellar ages, mean stellar metallicities and stellar mass, which have been used in this work to characterize the stellar populations of galaxies. The environment is defined by the local galaxy density estimated from a nearest neighbour approach, and by the distance to cluster centres obtained from a public catalogue of SDSS clusters. The main approach used in this study is the comparison of the relations between galaxy properties and environment for galaxies divided in intervals of luminosity and stellar mass. We summarize our main findings below.

(i) We recover the star formation–density relation in terms of the mean light-weighted stellar age, $\langle \log t_\star \rangle_L$, which is strongly correlated with star formation parameters derived from Hα emission line.

(ii) We confirm that high-density environments are populated by a large fraction of massive galaxies with old stellar populations, in opposition to low-density regions, dominated by low-mass galaxies actively forming stars. We also note that galaxies with intermediate stellar masses have constant fractions along the range of densities covered by our sample. The transition in galaxy fraction occurs at $\Sigma^t_{10} \sim 0.7\, h^2_{70}$ Mpc^{-2}, corresponding to 2–3 virial radii from cluster centres.

(iii) The environmental dependence of $\langle \log t_\star \rangle_L$ is distinct when we divide galaxies according to luminosity or stellar mass. The relation between mean age and local density is remarkable for galaxies in all bins of luminosity. On the other hand, only for an intermediate stellar mass interval (associated to a transition in galaxy properties) the relation shows a change in galaxy properties. For low-mass galaxies, the relation slightly increases along the density range, but showing low values of $\langle \log t_\star \rangle_L$ – characteristic of late-type galaxies – in all environments. The most-massive galaxies also show a slight change in the median values of $\langle \log t_\star \rangle_L$ as galaxy density increases, but their values are higher everywhere.

(iv) We find that the distinct behaviours of the *age–density relation* for galaxies divided by luminosity or stellar mass are associated to the large stellar mass of galaxies with the same luminosity in dense environments. In other words, the well-known star formation–density relation results from the prevalence of massive systems in high-density environments, independently of galaxy luminosity, in addition to the observed downsizing in galaxy formation, where the star formation is shifted from massive galaxies at early times to low-mass ones as the Universe evolves.

(v) A PCA of our parameter set reveals that the local galaxy density is primarily responsible for the total variance present in our data, whereas the mean light-weighted stellar age of galaxies is the secondary one. This result reflects that the age–density relation is the main driver of the environmental dependence observed in some galaxy properties.

(vi) The mean stellar metallicity of less-massive/luminous galaxies increases in high-density regions, indicating that even low-mass galaxies in dense environments tend to be more evolved than their counterparts in low-density regions.

(vii) Our results support that a natural path for galaxy evolution proceeds *via* a nurture way mainly at high redshifts: massive galaxies have been formed in denser regions and evolved in an accelerated way, contrasting with a more *unsocial* life of low-mass galaxies preferentially inhabiting low-density regions of the Universe.

In this work, the concept of 'nature via nurture' (see Ridley 2003, for a genetic view of this expression) in the scenario of galaxy evolution was advocated in order to summarize the results obtained here related to the environmental dependence of galaxy properties in the local Universe. Many steps are needed towards a comprehensive view of the processes which have guided galaxy formation and evolution, mainly those related to the properties of the stellar content of galaxies in high redshifts. We expect to contribute further to these issues in other papers of this series on Semi-Empirical Analysis of Galaxies.

ACKNOWLEDGMENTS

We thank the anonymous referee for comments and suggestions that helped improve this paper. We thank financial support from CNPq, FAPESP and the France–Brazil PICS programme. All the authors wish to thank the team of the SDSS for their dedication to a project which has made this work possible.

Funding for the SDSS has been provided by the Alfred P. Sloan Foundation, the Participating Institutions, the National Aeronautics and Space Administration, the National Science Foundation, the US Department of Energy, the Japanese Monbukagakusho, and the Max Planck Society. The SDSS is managed by the Astrophysical

Research Consortium (ARC) for the Participating Institutions. The Participating Institutions are The University of Chicago, Fermilab, the Institute for Advanced Study, the Japan Participation Group, The Johns Hopkins University, the Korean Scientist Group, Los Alamos National Laboratory, the Max-Planck-Institute for Astronomy (MPIA), the Max-Planck-Institute for Astrophysics (MPA), New Mexico State University, University of Pittsburgh, University of Portsmouth, Princeton University, the United States Naval Observatory, and the University of Washington.

REFERENCES

Adelman-McCarthy J. K. et al., 2006, ApJS, 162, 38
Baldry I. K., Glazebrook K., Brinkmann J., Ivezić Z., Lupton R. H., Nichol R. C., Szalay A. S., 2004, ApJ, 600, 681
Balogh M. L., Morris S. L., Yee H. K. C., Carlberg R. G., Ellingson E., 1999, ApJ, 527, 54
Balogh M. L., Baldry I. K., Nichol R., Miller C., Bower R., Glazebrook K., 2004, ApJ, 615, L101
Bardeen J. M., Bond J. R., Kaiser N., Szalay A. S., 1986, ApJ, 304, 15
Bekki K., Couch W. J., Shioya Y., 2001, PASJ, 53, 395
Benson A. J., Frenk C. S., Baugh C. M., Cole S., Lacey C. G., 2001, MNRAS, 327, 1041
Blanton M. R. et al., 2003a, ApJ, 594, 186
Blanton M. R., Lin H., Lupton R. H., Maley F. M., Young N., Zehavi I., Loveday J., 2003b, AJ, 125, 2276
Blanton M. R B. J., Csabai I., Doi M., Eisenstein D., Fukugita M., Gunn J. E., Hogg D. W., Schlegel D. J., 2003c, AJ, 125, 2348
Bravo-Alfaro H., Cayatte V., van Gorkon J. H., Balkowski C., 2000, AJ, 119, 580
Bruzual G., Charlot S., 2003, MNRAS, 344, 1000
Bundy K. et al., 2006, ApJ, 651, 120
Cardelli J. A., Clayton G. C., Mathis J. S., 1989, ApJ, 345, 245
Carter B. J., Fabricant D. G., Geller M. J., Kurtz M. J., McLean B., 2001, ApJ, 559, 606
Cen R., Ostriker J. P., 1993, ApJ, 417, 415
Chen H.-W., Marzke R. O., 2004, ApJ, 615, 603
Cid Fernandes R., Mateus A., Sodré L., Stasińska G., Gomes J. M., 2005, MNRAS, 358, 363 (SEAGal I)
Clemens M. S., Bressan A., Nikolic B., Alexander P., Annibali F., Rampazzo R., 2006, MNRAS, 370, 702
Cooper M. C., Newman J. A., Madgwick D. S., Gerke B. F., Yan R., Davis M., 2005, ApJ, 634, 833
Cowie L. L., Songaila A., Hu E. M., Cohen J. G., 1996, AJ, 112, 839
Davis M., Efstathiou G., Frenk C. S., White S. D. M., 1985, ApJ, 292, 371
De Lucia G., Springel V., White S. D. M., Croton D., Kauffmann G., 2006, MNRAS, 366, 499
Dressler A., 1980, ApJ, 236, 351
Dressler A., Gunn J. E., 1983, ApJ, 270, 7
Dressler A., Smail I., Poggianti B. M., Butcher H., Couch W. J., Ellis R. S., Oemler A. J., 1999, ApJS, 122, 51
Einasto J., Tago E., Einasto M., Saar E., Suhhonenko I., Heinämäki P., Hütsi G., Tucker D. L., 2005, A&A, 439, 45
Frenk C. S., White S. D. M., Efstathiou G., Davis M., 1985, Nat, 317, 595
Frenk C. S., White S. D. M., Davis M., Efstathiou G., 1988, ApJ, 327, 507
Fujita Y., Nagashima M., 1999, ApJ, 516, 619
Fukunaga K., 1990, Introduction to Statistical Pattern Recognition, 2nd edn. Academic Press, New York
Glazebrook K. et al., 2004, Nat, 430, 181
Gómez P. L. et al., 2003, ApJ, 584, 210
Goto T. et al., 2002, PASJ, 54, 515
Goto T. et al., 2003, PASJ, 55, 757
Gunn J. E., Gott J. R., 1972, ApJ, 176, 1
Guzman R., Gallego J., Koo D. C., Phillips A. C., Lowenthal J. D., Faber S. M., Illingworth G. D., Vogt N. P., 1997, ApJ, 489, 559
Hashimoto Y., Oemler A., Lin H., Tucker D. L., 1998, ApJ, 499, 589
Heavens A., Panter B., Jimenez R., Dunlop J., 2004, Nat, 428, 625
Hopkins A. M. et al., 2003, ApJ, 599, 971
Jimenez R., Panter B., Heavens A. F., Verde L., 2005, MNRAS, 356, 495
Juneau S. et al., 2005, ApJ, 619, L135
Kaiser N., 1984, ApJ, 284, L9
Kauffmann G. et al., 2003, MNRAS, 341, 33
Kauffmann G., White S. D. M., Heckman T. M., Ménard B., Brinchmann J., Charlot S., Tremonti C., Brinkmann J., 2004, MNRAS, 353, 713
Kennicutt R. C., 1998, ARA&A, 36, 189
Kewley L. J., Jansen R. A., Geller M. J., 2005, PASP, 117, 227
Kodama T. et al., 2004, MNRAS, 350, 1005
Larson R. B., Tinsley B. M., Caldwell C. N., 1980, ApJ, 237, 692
Lewis I. et al. (The 2dFGRS Team), 2002, MNRAS, 334, 673
Madau P., Ferrara A., Rees M. J., 2001, ApJ, 555, 92
Martin C. L., Kennicutt R. C., 2001, ApJ, 555, 301
Mateus A., Sodré L., 2004, MNRAS, 349, 1251
Mateus A., Sodré L., Cid Fernandes R., Stasińska G., Schoenell W., Gomes J. M., 2006, MNRAS, 370, 721(SEAGal II)
Menci N., Fontana A., Giallongo E., Salimbeni S., 2005, ApJ, 632, 49
Miller C. J., Nichol R. C., Gómez P. L., Hopkins A. M., Bernardi M., 2003, ApJ, 597, 142
Miller C. J. et al., 2005, AJ, 130, 968
Murtagh F., Heck A., 1987, Multivariate Data Analysis. Astrophys. Space Science Library. Reidel, Dordrecht
Poggianti B. M., Smail I., Dressler A., Couch W. J., Barger A. J., Butcher H., Ellis R. S., Oemler A., 1999, ApJ, 518, 576
Poggianti B. M. et al., 2006, ApJ, 642, 188
Ridley M., 2003, Nature via Nurture - Genes, Experience and What Makes us Human. Harper Collins Publishers, New York
Rines K., Geller M. J., Kurtz M. J., Diaferio A., 2005, AJ, 130, 1482
Scannapieco E., Ferrara A., Madau P., 2002, ApJ, 574, 590
Scannapieco E., Silk J., Bouwens R., 2005, ApJ, 635, L13
Schlegel D. J., Finkbeiner D. P., Davis M., 1998, ApJ, 500, 525
Sodre L., Cuevas H., 1997, MNRAS, 287, 137
Solanes J. M., Giovanelli R., Haynes M. P., 1996, ApJ, 461, 609
Steidel C. C., Adelberger K. L., Shapley A. E., Erb D. K., Reddy N. A., Pettini M., 2005, ApJ, 626, 44
Stoughton C. et al., 2002, AJ, 123, 485
Strateva I. et al., 2001, AJ, 122, 1861
Strauss M. A. et al., 2002, AJ, 124, 1810
Tanaka M., Goto T., Okamura S., Shimasaku K., Brinkmann J., 2004, AJ, 128, 2677
Tanaka M., Kodama T., Arimoto N., Okamura S., Umetsu K., Shimasaku K., Tanaka I., Yamada T., 2005, MNRAS, 362, 268
Thomas D., Maraston C., Bender R., de Oliveira C. M., 2005, ApJ, 621, 673
Tran K.-V. H., Franx M., Illingworth G., Kelson D. D., van Dokkum P., 2003, ApJ, 599, 865
Tully R. B., 2005, ApJ, 618, 214
Vollmer B., Cayatte V., Balkowski C., Duschl W. J., 2001, ApJ, 561, 708
Weinberg D. H., Davé R., Katz N., Hernquist L., 2004, ApJ, 601, 1
Whitmore B. C., Gilmore D. M., Jones C., 1993, ApJ, 407, 489.

This paper has been typeset from a TEX/LATEX file prepared by the author.